

Published in final edited form as:

Neurosci Lett. 2015 January 12; 585: 171–176. doi:10.1016/j.neulet.2014.12.004.

Long-term evaluation of Leber's hereditary optic neuropathy-like symptoms in rotenone administered rats

Li Zhang^{a,b}, Laura Liu^c, Ann L. Philip^b, Juan C. Martinez^b, Juan C. Gutierrez^b, Mathieu Marella^d, Gaurav Patki^d, Akemi Matsuno-Yagi^d, Takao Yagi^d, and Biju B. Thomas^{b,*}

^aEye Center, Second Affiliated Hospital, Medical School of Zhejiang University, Hangzhou, China

^bOphthalmology, Keck School of Medicine, University of Southern California, Los Angeles, CA

^cDepartment of Ophthalmology, Chang Gung Memorial Hospital, Linkou Medical Center, Taoyuan, Taiwan

^dMolecular and Experimental Medicine, The Scripps Research Institute, La Jolla, CA

Abstract

Leber's hereditary optic neuropathy (LHON) is an inherited disorder affecting the retinal ganglion cells (RGCs) and their axons that lead to the loss of central vision. This study is aimed at evaluating the LHON symptoms in rats administered with rotenone microspheres into the superior colliculus (SC). Optical coherence tomography (OCT) analysis showed substantial loss of retinal nerve fiber layer (RNFL) thickness in rotenone injected rats. Optokinetic testing in rotenone treated rats showed decrease in head-tracking response. Electrophysiological mapping of the SC surface demonstrated attenuation of visually evoked responses; however no changes were observed in the ERG data. The progressive pattern of disease manifestation in rotenone administered rats demonstrated several similarities with human disease symptoms. These rats with LHON-like symptoms can serve as a model for future investigators to design and implement reliable tests to assess the beneficial effects of therapeutic interventions for LHON disease.

Keywords

Leber's hereditary optic neuropathy; animal model; visual function; rotenone; superior colliculus

1. Introduction

Leber's Hereditary Optic Neuropathy (LHON) is a rare maternally inherited disorder caused by defects in complex I subunit of the mitochondrial respiratory chain. LHON is characterized by selective degeneration of the retinal ganglion cell (RGC) layer and rapid onset of visual loss [1, 2]. Clinically, LHON results in acute or subacute central visual

© 2014 Elsevier Ireland Ltd. All rights reserved.

*Corresponding to: Tel.: +1 323 442 5593 biju.thomas@med.usc.edu.

Publisher's Disclaimer: This is a PDF file of an unedited manuscript that has been accepted for publication. As a service to our customers we are providing this early version of the manuscript. The manuscript will undergo copyediting, typesetting, and review of the resulting proof before it is published in its final citable form. Please note that during the production process errors may be discovered which could affect the content, and all legal disclaimers that apply to the journal pertain.

failure, initially in one eye followed shortly by loss in the fellow eye [3-6]. During the acute stage, LHON presents a retinal nerve fiber layer (RNFL) edema, a chronic stage follows which is characterized by a preferential degeneration of central optic nerve fibers of the papillomacular bundle. As a result, a pronounced central or cecocentra scotoma is observed with retention of peripheral vision is typically noted in LHON patients [3-6]. At least 95% of individuals with LHON harbor one of three mutations in mtDNA (11778G>A, 14484T>C and 3460G>A) that affect genes encoding complex I subunit of the respiratory chain [3, 4, 7]. It is currently unknown why RGCs and optic nerve are preferentially affected, even though the mtDNA mutation is present throughout the body. And it is still unclear whether the disease is somagenic or axogenic as mitochondria are present both in the cell body and along the RGC axon [8]. Hence several factors pertaining to the origin and progression of the LHON disease still remain unclear. To develop effective treatment strategies and to better understand the disease mechanisms, it is important that faithful animal models presenting similarity with the human disease are created.

The majority of existing rodent models for LHON disease are created based on either direct injection of complex I inhibitor into the eye or genetic manipulation of complex I subunits [9-13]. Rotenone is a potent inhibitor of the mitochondrial complex I [14]. It has been used, in vitro and in vivo, to study neurodegenerative diseases [15, 16]. Dysfunction of the respiratory complex I lead to energy deficiency and excessive production of reactive oxygen species (ROS). Direct intravitreal injection of rotenone (0.5-1µl) induces rapid loss of RGCs followed by a reduced RNFL thickness observed as early as 24 hours after the injection as demonstrated by histological assessments [9-11]. In the above animal models, since the RGC body is the major target for disease induction, the chronic evolution that characterize the LHON diseases to be studied over a period of time could be missing. Hence the above approach may not be capable to provide sufficient window for therapy research. Another animal model created based on intravitreal administration of iRNA of complex I subunit of NDUFA1 also induced degeneration of RGCs; however no functional assay has been conducted [12]. A mutant mouse model, carrying mtDNA ND6 P25L mutation was reported more recently showing RGC axonal swelling and abnormal mitochondrial morphology [13]. These mice are also considered as a model for LHON disease although some deficiencies in photoreceptor function is observed based on ERG recording.

Our earlier studies demonstrated that subcutaneous injection of rotenone-loaded microspheres allow slow, persistent and long-term release of rotenone, resulting in a sustained level of rotenone in the blood for at least 2 months [17]. Based on this information a rat model showing LHON-like symptoms was created by rotenone microsphere administration in the optical layer of the superior colliculus (SC) [18]. In this model, both the nerve cells and their axons (especially node of Ranvier) are targeted instead of the whole retina and hence can be considered as a preferable model to study LHON-like disease symptoms [19]. Detailed visual functional analysis and imaging techniques are required to further establish that the above rat model manifests similarities with LHON patients in the progression and manifestation of the disease symptoms. Hence the present study is aimed to evaluate the disease symptoms of LHON in this animal model based on non-invasive imaging, behavioral and electrophysiological assessments and compare with disease symptoms in LHON patients.

2. Materials and Methods

2.1 Rotenone Microsphere Injection in Rats

Animals used in all experimental procedures were maintained in accordance with the NIH Guide for the Care, Use of Animals and the ARVO Statement for Use of Animals in Ophthalmologic and Vision Research, and with the approval of Animal Care and Use Committee (IACUC) of the USC. Fluorescent-tagged, biodegradable poly (DL-lactide-co-glycolide) (PLGA, lactide:glycolide 75:25, mol wt 90,000-126,000, Sigma) microsphere (50 μm diameter) beads loaded with either PBS or rotenone were used. Long Evans (LE) rats (Charles River Laboratories International, Wilmington, MA, USA) were housed in a 12 hours light/dark cycle. The LHON disease symptoms were induced by microinjection of rotenone-loaded PLGA microspheres (4 $\mu\text{g}/4 \mu\text{l}$) into the bilateral optical layer of the superior colliculus of anesthetized rats ($n=14$, 2-3 months old, male and female) at speed of 750 nl/min using a pump-driven 10ul Hamilton syringe. The location of injection was targeted based on stereotaxic coordinates established in our previous study [18]. Seven age-matched LE rats were injected with PBS-loaded PLGA microspheres as control group.

2.2 Optical Coherence Tomography (OCT)

Quantitative RNFL thickness measurements were obtained using Spectralis HRA2 + OCT (Heidelberg Engineering, Heidelberg, Germany). OCT images were segmented using software version 5.0 (Heidelberg Engineering, Heidelberg, Germany). RNFL thickness for each quadrant of the optic nerve head was averaged for the entire circumference around the optic disc (diameter of 3.4 mm). Mean RNFL and total retinal thickness were evaluated at 2, 4 and 8 weeks postoperatively.

2.3 Optokinetic (OKN) behavioral testing

Optokinetic testing was performed using a modified version of the custom-made computer based apparatus used previously [20]. The upgraded system is equipped with EthoVision® XT, Noldus Information Technology software that enabled easy recording and processing of the head-tracking behavior. Each rat was tested using a stripe width that evoked maximum head-tracking response based on previous experiments [20] and the total head-tracking duration was calculated for every 2 minutes test period. Contrast sensitivity was determined by varying the contrast of the black and white stripes. The animals were tested initially at the maximum contrast level (white:black=305:15 cd/m^2). The contrast sensitivity threshold for each animal was determined by decreasing the contrast between the black and white stripes at steps of approximately 0.5 cd/m^2 . The contrast at a given spatial frequency was calculated using the formula $(L_{\text{max}}-L_{\text{min}}) / (L_{\text{max}}+L_{\text{min}})$ where L_{max} is the brightness (in cd/m^2) of the white stripe, and L_{min} is the brightness of the black stripe (in cd/m^2). At each time point animals were tested 3 times.

2.4 Superior Colliculus (SC) Electrophysiology

Electrophysiological recordings of visual evoked responses in the SC were performed in anesthetized animals following overnight dark adaptation as described previously [21]. After unilateral parietal craniotomy, the SC was exposed by cortical suction. Under direct

visualization of the SC, a custom-made tungsten microelectrode was inserted superficially into the SC and advanced 200 microns below the surface. Recording was always started at the extreme lateral edge of the SC and was performed from up to 50 locations. The electrode was moved in definite rows and columns (approximately 200 microns apart) to cover the majority of the SC surface. During the recording of the visually evoked responses, a full field light flash of varying light intensity was projected onto the contralateral eye (Grass model PS 33 Photic stimulator, W. Warwick, RI, USA). The intensity of light stimulus was varied stepwise using neutral density filters (Lee Filters, Andover, U.K.) by a factor of 0.25 ranging from -6.44 to 0.19 log cd/m². Multi-unit responses were recorded using a PowerLab data acquisition system (ADI Instruments, Mountain View, CA, USA). Light evoked responses were averaged and analyzed using Scope software and the luminance threshold for each recording site was determined. The stereotactic co-ordinates of individual recording sites were plotted into a contour map using Origin Pro 8.6 (OriginLab, Northampton, MA) that represented the distribution of the threshold over the entire SC surface.

2.5 Electroretinography (ERG)

Rats were dark-adapted for a 12 hour period prior to ERG recordings performed using Espion ERG Diagnosys system (Diagnosys, Lowell MA). Animals were anesthetized with ketamine (75 mg/kg) and xylazine (1.0 mg/kg) anesthesia mixture administered intraperitoneally. The pupils were dilated using drops of 10% AK-Dilate (phenylephrine hydrochloride) and 0.5% tropicamide solution. Surface contact electrodes (Mayo Corporation, Japan) were placed on the rat eye with the help of Celluvisc (Allergan, Irvine, CA). Scotopic ERG analysis was performed using 0.001 to 10 cds/m² flash stimulus.

2.6 Statistical Analysis

Statistical comparisons were made with student's t-test using Graphpad Prism software (Graphpad Software Inc., La Jolla, CA). For all comparisons, the significance level was determined at $p < 0.05$.

3. Results

This study investigated the effect of rotenone administration on RNFL thickness by OCT imaging. After the infusion of rotenone microspheres bilaterally into the rat's optical layer of the SC, the animals exhibited one of the major characteristics of the LHON disease, a significant decrease ($p < 0.05$) in RNFL thickness (Fig. 1) that was observed at the 8 weeks post-injection period. No such defect was observed in the PBS injected control rats.

A decrease in the duration of head-tracking was observed in rotenone injected rats during the follow up assessments performed at various time points starting 2 weeks post-injection. The differences in the OKN response between rotenone treated and the PBS treated groups were found to be statistically significant during the 4, 6 and 8 week's post-injection tests ($p < 0.05$) (Fig. 2A). Rotenone treated animals also showed significant loss of contrast sensitivity when tested 8 week post-injection ($p < 0.05$) (Fig. 2B).

Electrophysiological recording from the superior colliculus demonstrated changes of the visual sensitivity in rotenone treated rats 8 weeks post-injection. The number of recording

sites that showed visually evoked responses during retinal light stimulation was significantly less in rotenone injected rats ($p < 0.05$). The decrease in the SC response was observed at the various light levels ($-6.44 \log \text{ cd/m}^2$ to $-0.39 \log \text{ cd/m}^2$) (Fig. 3A). A map of the SC showing threshold stimulus level suggested that the damage caused due to rotenone administration encompasses almost on the entire SC surface (Fig. 3 B).

Since the rodent retinas are composed of mostly rods [22], the scotopic ERG response after rotenone administration was evaluated. At 8 weeks, no significant defects were observed in the b-wave amplitude of rotenone injected and control animals. The oscillatory potentials (OPs) did not display any significant changes between rotenone and PBS injected rats.

4. Discussion

In humans, LHON disease induces a bilateral loss of vision that often occurs asynchronously over the course of several weeks [5, 6]. Some patients continue in a “chronic” disease state characterized by a low-grade degenerative process that may consistently worsen over time [6]. Here a method that induces, in rats, symptoms of LHON over a course of several weeks as to what it is observed in human during LHON progression is reported. This report describes a method that induces LHON symptoms in rats over a course of several weeks comparable to what is observed in human during disease progression.

Previous studies confirmed that ganglion cells are highly sensitive to the neurotoxic properties of rotenone in vivo [11]. Intravitreal delivery of rotenone could produce significant thinning of the nerve fiber, inner plexiform and ganglion cell layers, and loss of RGC 1-7 days post- intravitreal injection [9-11]. In the rat model reported in this study, the injection of slow releasing rotenone-loaded microspheres directly into the optic layer of the superior colliculus triggered optic nerve atrophy and concomitant functional deficits. The above symptoms are comparable to the observations in human LHON patients.

Multiple visual functional assessments were used (OCT, ERG, contrast sensitivity assessments and recording from the higher visual centers) that are comparable to the standard clinical assessments performed in LHON patients [23-27]. Infusion of rotenone containing microspheres into the rat superior colliculus will cause rotenone uptake by mitochondria at the optic nerve axonal terminals by its retrograde transport since it has been well established that mitochondria can move in both anterograde and retrograde directions in one axon [28]. The animal model reported here displayed progressive rotenone-induced RNFL thickness loss and visual functional deficits suggesting that this model could be used to test treatment strategies at desirable stages of the disease progression.

OCT assessment clearly demonstrated loss of RNFL thickness that can be considered a typical manifestation of the human disease condition [23]. Although OCT scanning in our rat model demonstrated considerable loss of RNFL thickness, there was no sign of pseudoedema or papilledema – the anomalies observed in the human patients [4, 25]. Such discrepancies can be expected due to the fundamental differences in the structure between human and rodent eyes.

Visual functional assessments are important measures to understand the beneficial effects of treatment strategies employed in animal disease models. Optokinetic (OKN) testing is a fast and reliable testing procedure that could be easily repeated several times in the same animal at different time points after treatment [20]. Statistically a significant decrease in the duration of optokinetic head-tracking response was observed in rotenone treated rats. Based on our previous observations, damage to the retina and optic nerve starts about 2 weeks post-injection which leads to vision impairment mostly due to the degeneration by ROS [18, 19]. Some discrepancy observed in the OKN score between the current investigation and the previous study could be related to the possible differences in the OKN scoring procedures employed in the two different laboratories.

Additional defects in the visual function of rotenone treated rats were observed based on the contrast sensitivity data. Loss of contrast sensitivity is considered a manifestation of the inner retinal defects [29]. Rotenone injected rats showed contrast sensitivity defects when tested at various luminance conditions suggesting the severity of the disease progression. This finding is also in consistent with clinical study data demonstrating contrast sensitivity loss in LHON patients [24].

Pattern ERG (pERG) is considered a useful tool for assessing functional changes at the level of ganglion cells in LHON patients, in this animal study, the properties of the visual signals from ganglion cell terminations based on superior colliculus electrophysiology were investigated. Significant differences between rotenone injected and PBS-injected animals were observed in the properties of visual signals reaching the higher visual area of the brains. As shown in Fig. 3A, at lower stimulus levels, only few SC sites in rotenone injected animals showed responses to light stimulation. Considering the significant RNFL thickness loss observed in the rotenone treated animals, the SC electrophysiology data suggests possible damage occurred at the level of inner retinal layers including the axons of the ganglion cells. The retina, which is an extension of the central nervous system, has the highest relative oxygen demand compared to any other tissue in the body [3, 7]. This renders it exceedingly susceptible to mitochondrial dysfunction. Rotenone uptake could take place in the area immediately surrounding the injection site, the deleterious effects of rotenone could be extended to distal areas and eventually the damage could be more global. This is supported by the SC mapping data demonstrating damage extended to the central and cecocentral regions of the superior colliculus. This finding is largely in accordance with clinical observation in LHON patients showing characteristic central or cecocentral scotoma [25, 26].

Finally, the electrophysiological testing based on ERG b-wave amplitude and oscillatory potential suggested no apparent differences between rotenone and PBS injected animals. The above finding demonstrates that most of the retinal function remained unaffected due to rotenone induced atrophy and the disease manifestation is more limited to the RGC function. No a-wave results are presented here since it is assumed that rotenone mostly affected the RGCs. ERG studies in LHON patients also demonstrated apparent absence of defects in the ERG wave forms [27] indicating functional integrity of photoreceptors, bipolar cells and müller cells.

In summary, the current study demonstrates the progressive pattern of LHON-like disease symptoms in rotenone administered rats and its similarities with the human disease condition. The LHON-like rats presented here may help future investigators to design and implement reliable tests for assessing the beneficial effects of therapeutic agents.

Acknowledgments

This work was supported by NIH grant (R01EY020796) and an Unrestricted Departmental grant from Research to Prevent Blindness, New York, NY 10022 to USC Department of Ophthalmology.

References

1. Howell N. Leber hereditary optic neuropathy: mitochondrial mutations and degeneration of the optic nerve. *Vision Res.* 1997; 37:3495–3507. [PubMed: 9425526]
2. Man PY, Turnbull DM, Chinnery PF. Leber hereditary optic neuropathy. *J Med Genet.* 2002; 39:162–169. [PubMed: 11897814]
3. Carelli V, Ross-Cisneros FN, Sadun AA. Mitochondrial dysfunction as a cause of optic neuropathies. *Prog Retin Eye Res.* 2004; 23:53–89. [PubMed: 14766317]
4. Fraser JA, Biousse V, Newman NJ. The neuro-ophthalmology of mitochondrial disease. *Surv Ophthalmol.* 2010; 55:299–334. [PubMed: 20471050]
5. Yen MY, Wang AG, Wei YH. Leber's hereditary optic neuropathy: a multifactorial disease. *Prog Retin Eye Res.* 2006; 25:381–396. [PubMed: 16829155]
6. Sadun AA, Salomao SR, Berezovsky A, Sadun F, Denegri AM, Quiros PA, Chicani F, Ventura D, Barboni P, Sherman J, Sutter E, Belfort R Jr, Carelli V. Subclinical carriers and conversions in Leber hereditary optic neuropathy: a prospective psychophysical study. *Trans Am Ophthalmol Soc.* 2006; 104:51–61. [PubMed: 17471325]
7. Brandon MC, Lott MT, Nguyen KC, Spolim S, Navathe SB, Baldi P, Wallace DC. MITOMAP: a human mitochondrial genome database--2004 update. *Nucleic Acids Res.* 2005; 33:D611–613. [PubMed: 15608272]
8. Levin LA. Axonal loss and neuroprotection in optic neuropathies. *Can J Ophthalmol.* 2007; 42:403–408. [PubMed: 17508035]
9. Zhang X, Jones D, Gonzalez-Lima F. Mouse model of optic neuropathy caused by mitochondrial complex I dysfunction. *Neurosci Lett.* 2002; 326:97–100. [PubMed: 12057837]
10. Heitz FD, Erb M, Anklin C, Robay D, Pernet V, Gueven N. Idebenone protects against retinal damage and loss of vision in a mouse model of Leber's hereditary optic neuropathy. *PLoS One.* 2012; 7:e45182. [PubMed: 23028832]
11. Rojas JC, Saavedra JA, Gonzalez-Lima F. Neuroprotective effects of memantine in a mouse model of retinal degeneration induced by rotenone. *Brain Res.* 2008; 1215:208–217. [PubMed: 18486118]
12. Qi X, Lewin AS, Hauswirth WW, Guy J. Suppression of complex I gene expression induces optic neuropathy. *Ann Neurol.* 2003; 53:198–205. [PubMed: 12557286]
13. Lin CS, Sharpley MS, Fan W, Waymire KG, Sadun AA, Carelli V, Ross-Cisneros FN, Baciup P, Sung E, McManus MJ, Pan BX, Gil DW, Macgregor GR, Wallace DC. Mouse mtDNA mutant model of Leber hereditary optic neuropathy. *Proc Natl Acad Sci U S A.* 2012; 109:20065–20070. [PubMed: 23129651]
14. Singer TP, Ramsay RR. The reaction sites of rotenone and ubiquinone with mitochondrial NADH dehydrogenase. *Biochim Biophys Acta.* 1994; 1187:198–202. [PubMed: 8075112]
15. Betarbet R, Sherer TB, MacKenzie G, Garcia-Osuna M, Panov AV, Greenamyre JT. Chronic systemic pesticide exposure reproduces features of Parkinson's disease. *Nat Neurosci.* 2000; 3:1301–1306. [PubMed: 11100151]
16. Cabezas R, El-Bacha RS, Gonzalez J, Barreto GE. Mitochondrial functions in astrocytes: neuroprotective implications from oxidative damage by rotenone. *Neurosci Res.* 2012; 74:80–90. [PubMed: 22902554]

17. Marella M, Seo BB, Nakamaru-Ogiso E, Greenamyre JT, Matsuno-Yagi A, Yagi T. Protection by the NDI1 gene against neurodegeneration in a rotenone rat model of Parkinson's disease. *PLoS One*. 2008; 3:e1433. [PubMed: 18197244]
18. Marella M, Seo BB, Thomas BB, Matsuno-Yagi A, Yagi T. Successful amelioration of mitochondrial optic neuropathy using the yeast NDI1 gene in a rat animal model. *PLoS One*. 2010; 5:e11472. [PubMed: 20628600]
19. Marella M, Patki G, Matsuno-Yagi A, Yagi T. Complex I inhibition in the visual pathway induces disorganization of the node of Ranvier. *Neurobiol Dis*. 2013; 58:281–288. [PubMed: 23816754]
20. Thomas BB, Shi D, Khine K, Kim LA, Satta SR. Modulatory influence of stimulus parameters on optokinetic head-tracking response. *Neurosci Lett*. 2010; 479:92–96. [PubMed: 20488227]
21. Thomas BB, Seiler MJ, Satta SR, Aramant RB. Superior colliculus responses to light - preserved by transplantation in a slow degeneration rat model. *Exp Eye Res*. 2004; 79:29–39. [PubMed: 15183098]
22. Jeon CJ, Strettoi E, Masland RH. The major cell populations of the mouse retina. *J Neurosci*. 1998; 18:8936–8946. [PubMed: 9786999]
23. Barboni P, Savini G, Valentino ML, Montagna P, Cortelli P, De Negri AM, Sadun F, Bianchi S, Longanesi L, Zanini M, de Vivo A, Carelli V. Retinal nerve fiber layer evaluation by optical coherence tomography in Leber's hereditary optic neuropathy. *Ophthalmology*. 2005; 112:120–126. [PubMed: 15629831]
24. Ventura DF, Quiros P, Carelli V, Salomao SR, Gualtieri M, Oliveira AG, Costa MF, Berezovsky A, Sadun F, de Negri AM, Sadun AA. Chromatic and luminance contrast sensitivities in asymptomatic carriers from a large Brazilian pedigree of 11778 Leber hereditary optic neuropathy. *Invest Ophthalmol Vis Sci*. 2005; 46:4809–4814. [PubMed: 16303983]
25. Hudson G, Yu-Wai-Man P, Chinnery PF. Leber hereditary optic neuropathy. *Expert Opin Med Diagn*. 2008; 2:789–799. [PubMed: 23495818]
26. Warner RB, Lee AG. Leber hereditary optic neuropathy associated with use of ephedra alkaloids. *Am J Ophthalmol*. 2002; 134:918–920. [PubMed: 12470769]
27. Shibata K, Shibagaki Y, Nagai C, Iwata M. Visual evoked potentials and electroretinograms in an early stage of Leber's hereditary optic neuropathy. *J Neurol*. 1999; 246:847–849. [PubMed: 10525988]
28. Saxton WM, Hollenbeck PJ. The axonal transport of mitochondria. *J Cell Sci*. 2012; 125:2095–2104. [PubMed: 22619228]
29. Cursiefen C, Horn F, Junemann AGM, Korth M. Reduced recovery of temporal contrast sensitivity after flicker stress in patients with glaucoma. *J Glaucoma*. 2000; 9:296–302. [PubMed: 10958602]

Highlights

- Loss of visual function in rats after rotenone injection in the superior colliculus
- Behavioral and electrophysiological data comparable to human clinical symptoms
- Rotenone injection into rat superior colliculus serves as a model for LHON study

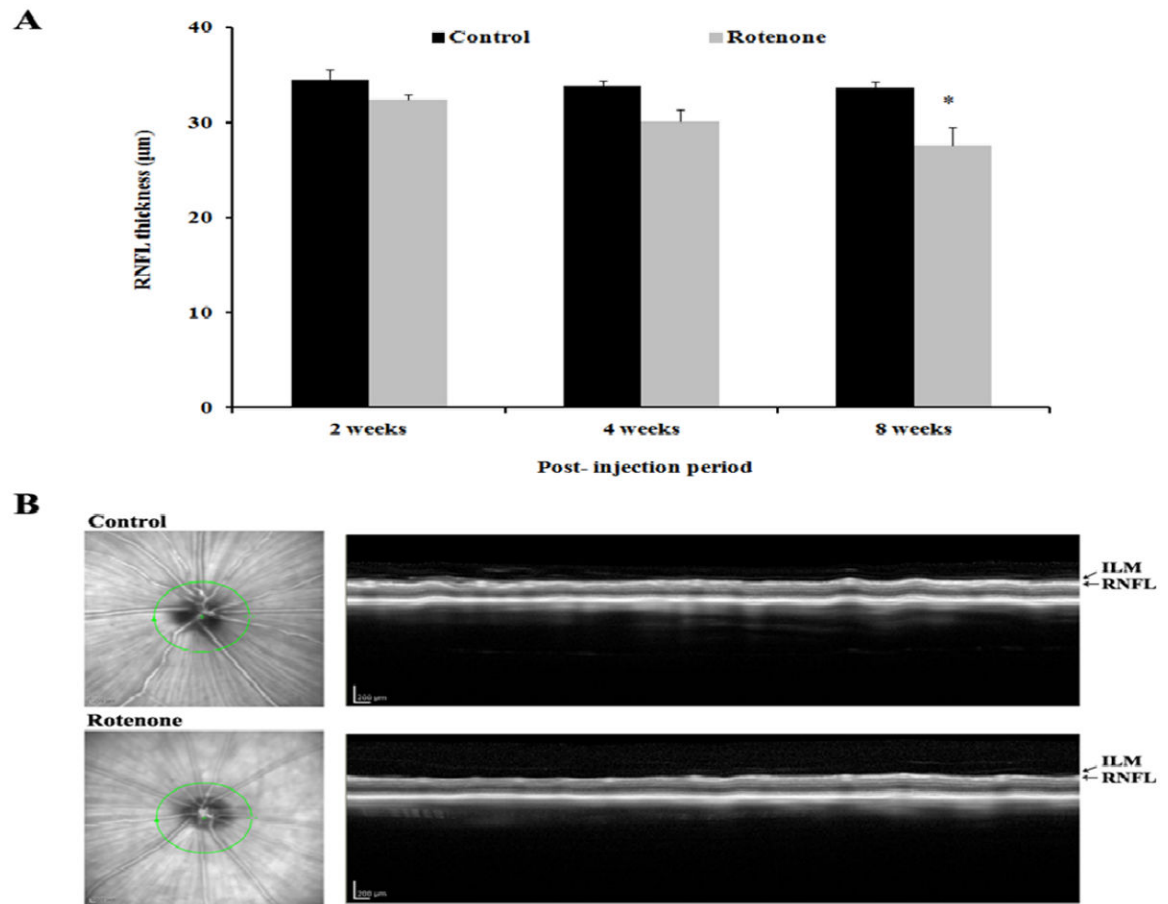


Fig.1. (A) Mean retinal nerve fiber layer (RNFL) thickness (mean \pm SEM) of control (n=7) and rotenone (n=14) injected rats at various time points after rotenone administration in the superior colliculus. Significant differences between the groups in the RNFL thickness is indicated with * ($p<0.05$). (B) Representative OCT image of a control and a rotenone injected rat at 8 weeks after injection. ILM: inner limiting membrane.

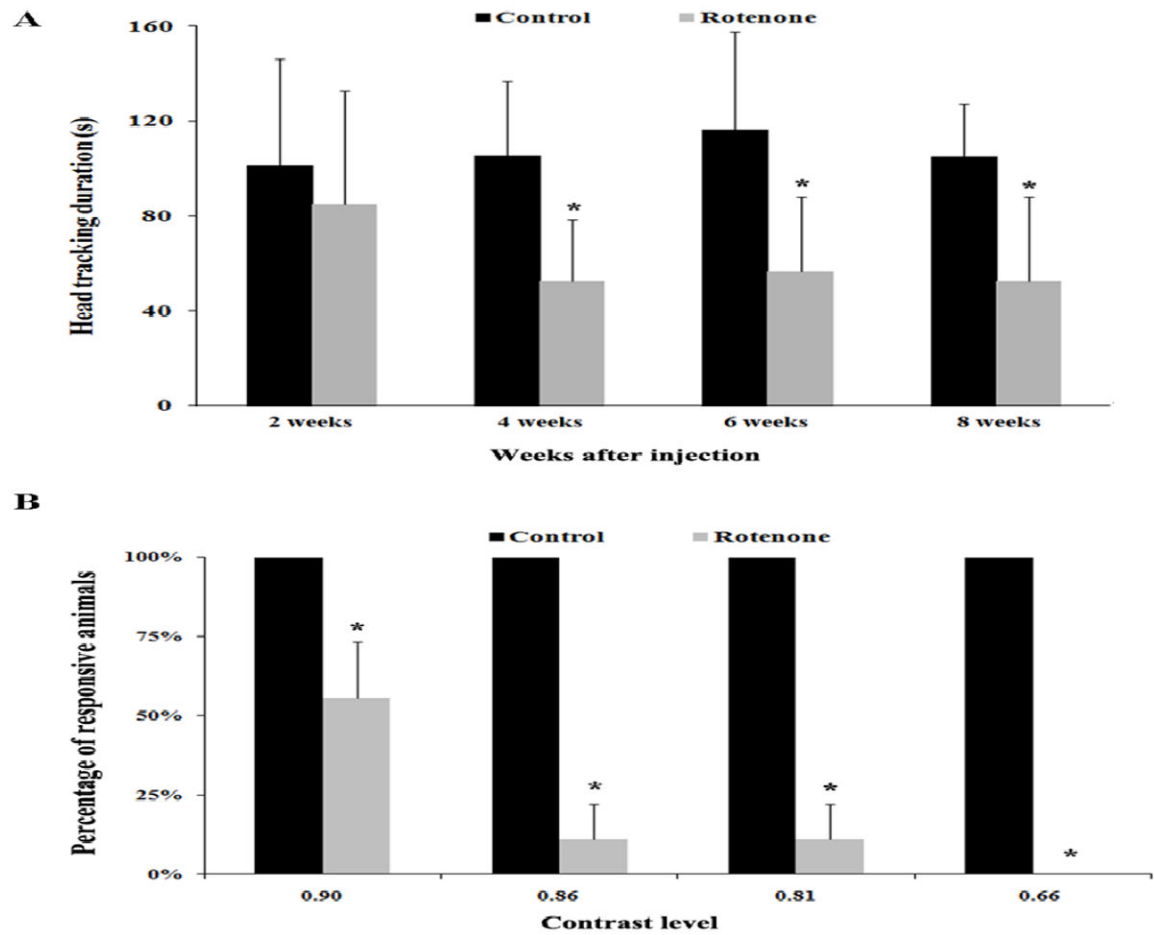


Fig. 2. (A) Optokinetic head-tracking duration (mean \pm SEM) of control (n=7) and rotenone (n=14) injected groups at various time points after administration of rotenone in the superior colliculus. Measurements were made at a luminance level of 0.22 log cd/m². (B) Differences in the contrast sensitivity (mean \pm SEM) between control (n=7) and rotenone injected rats (n=14) measured at 8 weeks post administration of rotenone in the superior colliculus. Significant differences between the groups are indicated with * (p<0.05).

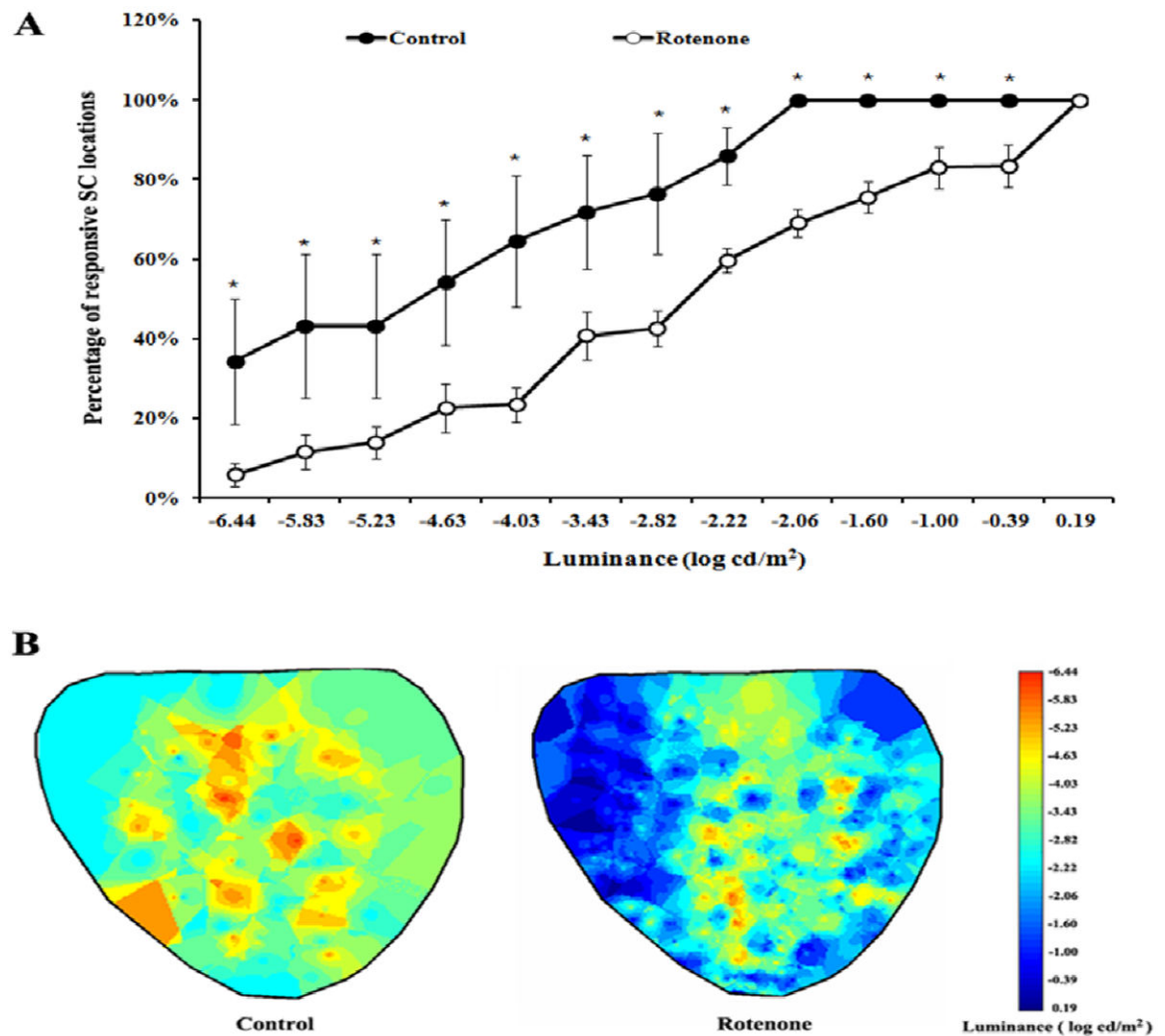


Fig. 3. (A) Percentage of responsive SC areas (mean±SEM) at various light stimulus used for retinal stimulation in control (n=5) and rotenone (n=8) injected groups. Significant differences between the two groups (* $p < 0.05$) in the stimulus threshold is observed throughout the SC surface. The recordings were made from up to 50 SC locations. (B) Representative diagrammatic sketch of the SC map showing stimulus threshold at various recording sites from a control animal (left) and a rotenone treated animal (right).

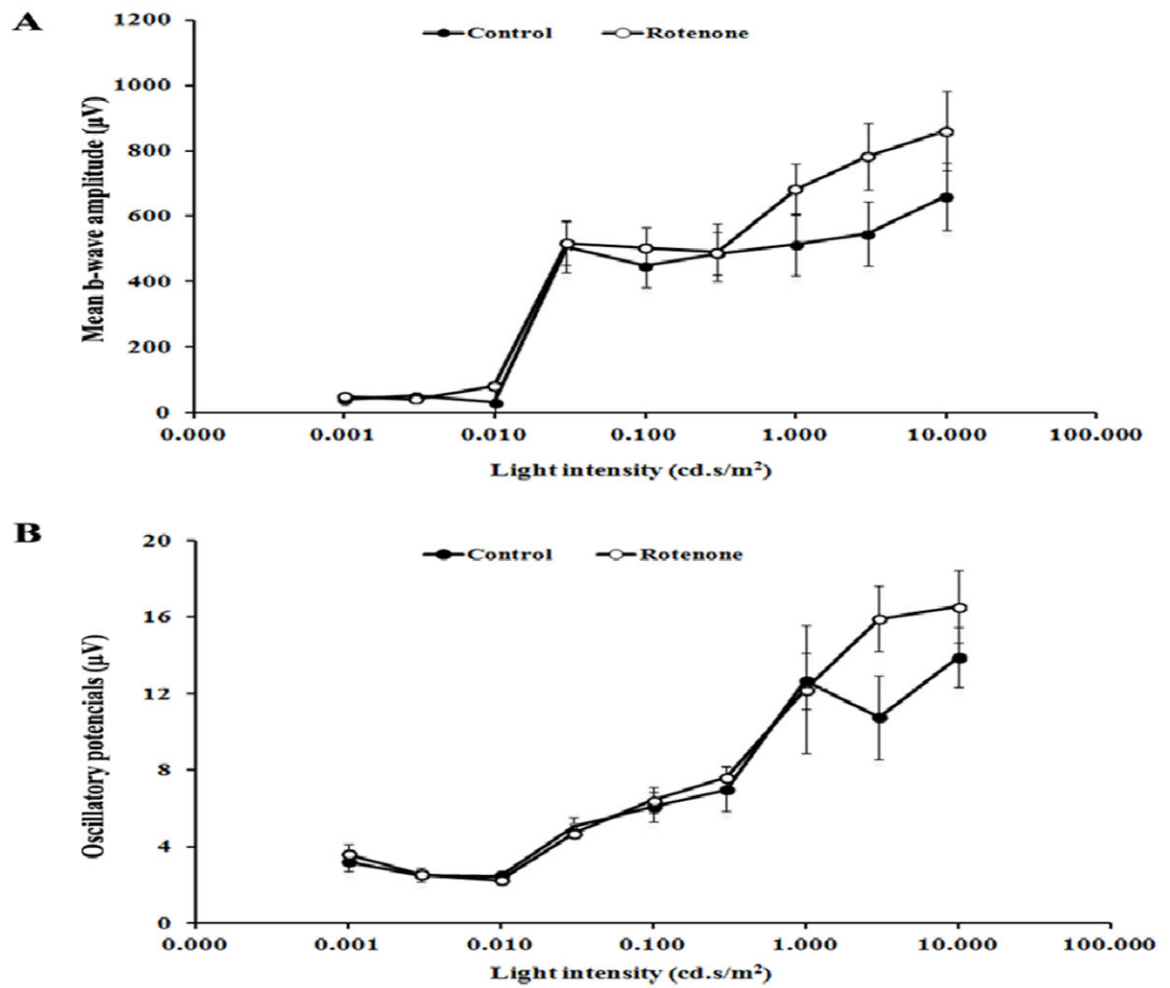


Fig. 4. (A) ERG b-wave amplitudes (mean±SEM) and (B) oscillatory potential (mean±SEM) of control group (n=4) and rotenone (n=6) injected group. No significant differences ($p>0.05$) were observed between the control and rotenone treated animals tested at 8 weeks post-injection.